Fuel cells technologies for wireless MEMS

2

H. Ren, J. Chae
Arizona State University, Tempe, AZ, United States

2.1 Introduction

2.1.1 Fuel cell fundamentals

Fuel cells are energy converters that directly convert chemical energy stored within fuels into electricity. A fuel cell is one of the most important energy converters and has the advantage of high conversion efficiency and high reliability. According to the U.S. Department of Energy, fuel cells achieve an efficiency of 42–53% at full power output [1], and according to Sure Power Corporation, one of their power systems based on phosphoric acid fuel cells guarantees 99.9999% reliability [2]. Currently, fuel cells also have a large, growing market globally. According to a report in 2013 by Fuel Cells 2000, it is estimated that at least 170 MW of fuel cells were installed in the United States in 2013, implemented for data centers, telecom towers, materials handling equipment, etc. [2].

Since its origins, a variety of fuel cells have been developed, including polymer electrolyte membrane fuel cells (PEMFC), solid oxide fuel cells (SOFC), hydrogen fuel cells (HFC), and biofuel cells (including microbial fuel cells (MFCs)). Fig. 2.1 shows a schematic of a general two-chamber fuel cell, which consists of anode and cathode chambers separated by an ion exchange membrane [3]. The anode and cathode are located in the corresponding chambers. Fuels, such as hydrogen, are in the anode chamber while oxidation materials, such as oxygen, are located in the cathode chamber. During operation, the hydrogen is oxidized while the oxygen is reduced, and electrons are generated during this process.

2.1.1.1 Voltage generation

Voltage output is a critical parameter for a fuel cell, and the voltage across the anode and cathode of a fuel cell can be determined by the electrochemical potential of the anode and cathode:

$$E = E_c - E_a \tag{2.1}$$

For instance, in a MFC, when the anode chamber is acetate and the cathode chamber is oxygen, the anode and cathode potentials are −0.284 and 0.805 V versus a standard hydrogen electrode (SHE), respectively. Thus, the open circuit voltage of the MFC is 1.089 V. As a comparison, a HFC, which utilizes hydrogen in the anode chamber and

Wireless MEMS Networks and Applications. http://dx.doi.org/10.1016/B978-0-08-100449-4.00002-6

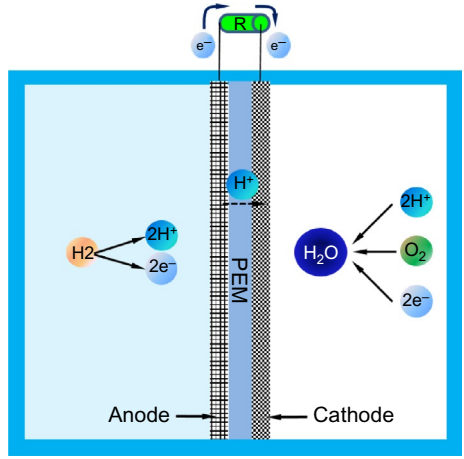

Fig. 2.1 Schematic of a typical two-chamber fuel cell. Here, the anolyte is hydrogen and the catholyte is oxygen as an example. During operation, hydrogen is oxidized at the anode chamber and protons pass through the proton exchange membrane (PEM) to reduce the oxygen at the cathode chamber.

oxygen in the cathode chamber, has anode and cathode potentials of 0 and 1.229 V versus SHE respectively; thus, the open circuit voltage of a HFC is 1.229 V.

2.1.1.2 Efficiency

Efficiency is another critical parameter for fuel cells, and it represents the number of electrons or the amount of energy stored inside the fuel converted by the fuel cell. Efficiency is generally classified as columbic efficiency (CE) and energy conversion efficiency; the former is a measure of the percentage of electrons converted, while the latter is a measure of the percentage of energy converted.

Columbic efficiency

CE is a measure of the percentage of electrons converted by a fuel cell, and Eq. (2.2) is used to calculate CE:

$$\mathrm{CE} = \frac{C_\mathrm{P}}{C_\mathrm{T}} \times 100\% \tag{2.2}$$

where C_P is the total coulombs calculated by integrating the current over the time for the fuel consumption, and C_T is the maximum possible coulombs of the fuel.

Energy efficiency

Energy efficiency (EE) is a measure of the proportion of energy converted by a fuel cell, and Eq. (2.3) is used to calculate EE:

$$\mathrm{EE} = \frac{E_\mathrm{P}}{E_\mathrm{T}} \times 100\% \tag{2.3}$$

where E_P is the total energy calculated by integrating the power output over the time for fuel, and E_T is the maximum possible energy of the fuel.

2.1.2 Micro-electromechanical systems for fuel cells

MEMS stands for micro-electromechanical systems, and it has been a technological and commercial success during the past three decades, with accelerometers, gyroscopes, pressure sensors, digital micro-mirror devices, etc. being successfully commercialized [3–7]. The attractive features of MEMS, which have led to its commercial success, include small size, light weight, cost effective batch fabrication, and precision control of physical dimensions. These features have also benefited a variety of MEMS-based fuel cells, including micro polymer electrolyte fuel cells, micro direct methanol fuel cells (DMFCs), micro SOFCs, micro biofuel cells, etc. Unlike traditional fuel cells, the MEMS fuel cells are characterized by high-power density, high surface area to volume ratio, and improved mass transfer [3].

2.1.3 Wireless MEMS systems

Wireless MEMS systems, such as wireless sensor networks and internet of things (IoT) [8,9], have emerged in the past few decades, covering wide applications in areas including healthcare monitoring, environmental monitoring, and industrial monitoring. The power sources for wireless systems holds the bottleneck of demand to follow the scaling effect of complementary metal–oxide–semiconductor (CMOS), and they currently occupy the largest footprint in a wireless sensor network [10]. Furthermore, the power source determines the operational life time of a node in the wireless sensor network [10]. This directly demands high energy density for power sources of wireless sensor networks, where fuel cells excel. For example, methanol has an energy density of 17.6 kJ cm^{-3}, which is approximately six times that of a lithium battery. Therefore, it is essential to develop high performance fuel cells for wireless systems. Most wireless systems require a power ranging from hundreds of μW to hundreds of mW. Some ultra-low wireless systems also exist, in the range of sub 10 μW wireless systems [11]. Thus, fuel cell designs need to accommodate the varying power demand of wireless systems. In the next three sections, we will discuss the three major fuel cells that have been mainly studied in the last five decades.

2.2 Polymer electrolyte membrane fuel cells

2.2.1 PEMFC fundamentals

2.2.1.1 Operation principle

Polymer electrolyte membrane fuel cells (PEMFC), also referred to as proton exchange membrane fuel cells (PEMFC), utilize polymer electrolyte membranes (PEMs), such as Nafion, to conduct protons for ion exchange purposes. PEMFC

consumes mainly hydrogen, methanol, or formic acid [12]. During operation, the hydrogen, methanol, or formic acid in the anode chamber is oxidized while the oxygen in the cathode chamber is reduced.

PEMFC was first invented in the early 1960s by General Electric for NASA in the Gemini spacecraft. Despite their successful technical demonstration, the difficulty of management and high cost impeded the further development until the 1990s, when reliable PEM was implemented. Low-cost catalysts were adopted and electrode/membrane configurations improved to greatly reduce the overall cost (eg, the amount of platinum used in PEMFC reduced by 10–100 fold) [13]. Currently, the power density of PEMFC reaches up to 0.5–0.7 W cm^{-2}.

2.2.2 MEMS-based PEMFC

Since 2000, a variety of MEMS-based PEMFC have been studied. Fig. 2.2 gives an overview of the different MEMS PEMFCs reported in the literature. In 2000, Kelley et al. [20] reported a miniaturized methanol/air polymer electrolyte fuel cell on silicon substrate with an active area of 0.25 cm^2, delivering a current density of 0.1 mA cm^{-2} at 90°C. Lee et al. [14] presented a flip-flop configuration with a power density of 40 mW cm^{-2} for an integrated series connection of polymer electrolyte fuel cells in a planar array in 2003. A hydrogen-air micro PEMFC on silicon and polydimethylsiloxane (PDMS) base substrates was presented by Shah et al. [15] marking a current density of 18 mA cm^{-2} at 40°C in 2004. In 2006, Yao et al. reported a high-power density, silicon-based microscale DMFC. This work implemented a silicon wafer with arrays of etched holes selectively coated with a nonwetting agent to collect water at the cathode, a silicon membrane micro pump to pump the collected water back to the anode, and a passive liquid–gas separator to remove CO_2. The attractive features of this fuel cell include completely microfabricated silicon-based components in a monolithic manner, minimizing interconnects and integration costs [21]. Zhang et al. [16] presented a miniaturized 6-cell PEMFC stack fabricated by a microfabrication technique with a power density of 104 mW cm^{-2} for each cell, delivering a stack voltage of 5.3 V. In 2009, Kim and Kwon presented a MEMS fuel cell system aiming for a portable power source. All the components, including a methanol–steam reformer, catalytic combustor, preferential oxidation (PROX) reactor, and PEMFC, were fabricated by standard microfabrication techniques [17], presenting a power density of 195 mW cm^{-2}. Peng et al. [18] integrated micro/nano synergical structures in a MEMS PEMFC to improve the efficiency of PEMFC to a best efficiency of a catalyst utilization ratio of 38.2W g_{pt}^{-1}, which can be considered among the best performed micro-fuel cells. In 2014, a microscale space power system using PEMFC was developed for nano-satellites by Lee and Kim. The fuel cell used sodium borohydride ($NaBH_4$) and hydrogen peroxide (H_2O_2) as a hydrogen and oxygen source, respectively [19].

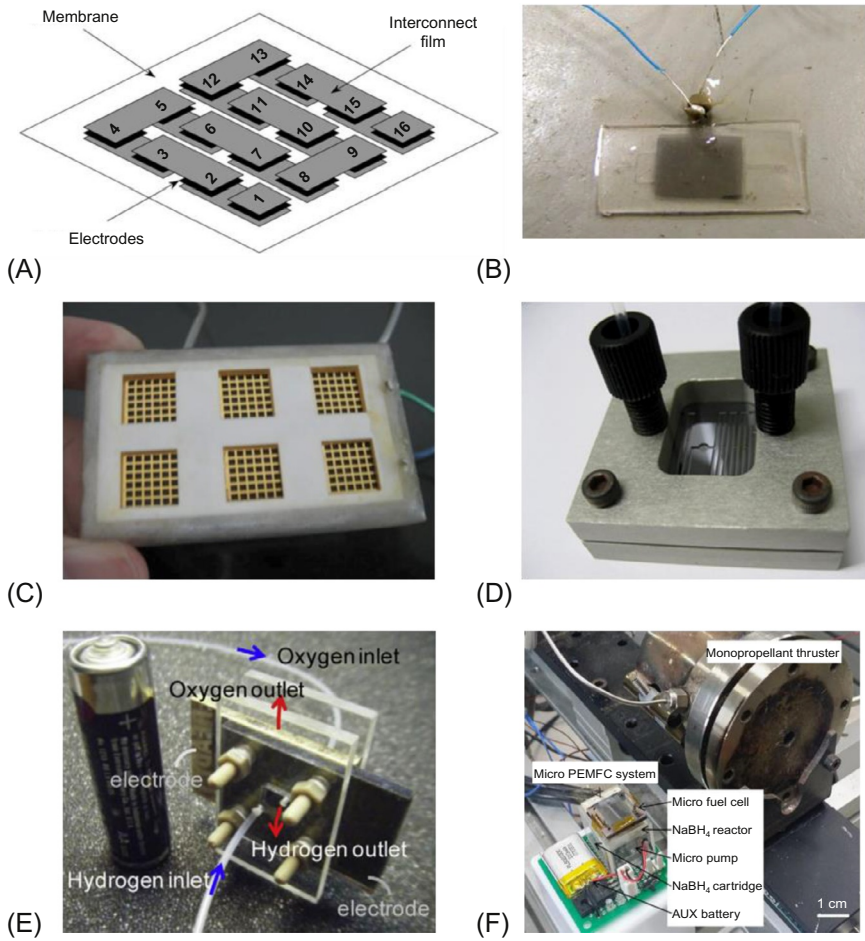

Fig. 2.2 Various MEMS PEMFCs reported in the literature: (A) schematic of a flip-flop MEMS PEMFC planar array presented by Lee et al. [14]; (B) optical image of a hydrogen-air micro PEMFC on silicon and polydimethylsiloxane (PDMS) base substrates presented by Shah et al. [15]; (C) optical image of a miniaturized 6-cell PEMFC stack presented by Zhang et al. [16]; (D) optical image of a MEMS fuel cell system for application as a portable power source by presented by Kim and Kwon in 2010 [17]; (E) optical image of a MEMS PEMFC integrated with micro/nano structures by Peng et al. [18]; (F) optical image of a micro PEMFC system combined with an $NaBH_4$ hydrogen generator by Lee and Kim in 2014 [19].

2.3 High temperature fuel cells

2.3.1 SOFC fundamentals

An SOFC utilizes a solid ion exchange membrane for ion exchange. It operates at high temperatures between 500°C and 1000°C. The high operation temperatures allow avoidance of an expensive catalyst, ie, platinum-based catalyst. Fig. 2.3 shows a schematic of SOFC. SOFC consists of three layers: anode, solid ion exchange membrane, and cathode. During operation, hydrogen is oxidized at the anode while oxygen is reduced at the cathode. The reduced oxygen migrates across the solid electrolyte to the anode, and water is formed as a by-product.

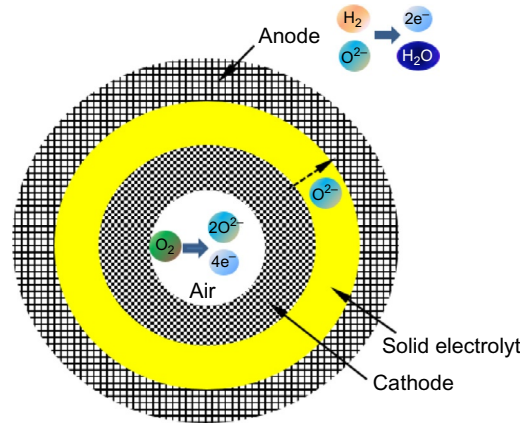

Fig. 2.3 Schematic of an SOFC, which is composed of three layers: anode, solid electrolyte, and cathode. During operation, oxygen is reduced at the cathode, and O^{2-} ions go through the solid electrolyte; O^{2-} ions react with hydrogen to form water at the anode.

The idea of SOFC can date back to the 1890s when Nernst first described a composition of 85% zirconium oxide and 15% yttrium oxide as an ion conductor [22]. In 1935, Schottky [22] suggested that zirconium oxide and yttrium oxide could be utilized for solid electrolyte for fuel cells. SOFC has become an active research area during the past few decades.

2.3.2 MEMS-based SOFC

Fig. 2.4 gives an overview of MEMS-based SOFCs reported in the literature. Srikar et al. reported one of the early MEMS-based SOFC in 2003. They evaluated the effect of electrolyte thickness on the fuel cell performance with a simple analytical model and proposed a unique design of MEMS SOFC [27]. A self-supporting electrolyte membrane for SOFC was presented by Baertsch et al. [28], who fabricated submicron dense nanocrystalline yttria-stabilized zirconia and gadolinium-doped ceria film on a silicon nitride membrane using electron beam evaporation and sputtering, with selective silicon nitride removal leaving a free-standing, square electrolyte membrane. In 2006, Ahn et al. [23] reported a single-chamber SOFC with a micropatterned

interdigitated electrode delivering a power density of 73.5 mW cm^{-2} at 900°C. An ultrathin SOFC-containing electrolyte membrane of 50–150 nm thick was fabricated by sputtering, lithography, and etching. The SOFC operates at a low temperature of 350–400°C, producing 400 mW cm^{-2} [24]. Bieberle-Hütter et al. [29] reported a MEMS-based SOFC equipped with positive electrode–electrolyte–negative electrode multilayer membrane on Foturan and Si substrate. The MEMS-based SOFC delivered 150 mW cm^{-2}. Su et al. [25] reported an SOFC with corrugated thin-film electrolyte. In order to increase the electrochemical surface area, a yttria-doped $SrTiO_3$ (YST) membrane with a thickness of 70 nm was deposited on prepatterned silicon to form a corrugated pattern, and power densities of the corrugated fuel cells of 677 and 861 mW cm^{-2} were obtained at 400°C and 450°C, respectively. In another study, they fabricated corrugated thin-film electrolyte membranes by nanosphere lithography and atomic layer deposition and achieved a power density of 1.34 W cm^{-2} at 500°C [30]. In 2011, Tsuchiya et al. [26] presented a nanostructured membrane with lateral dimensions on the scale of millimeters or centimeters for MEMS SOFC and achieved a power density of 155 mW cm^{-2}.

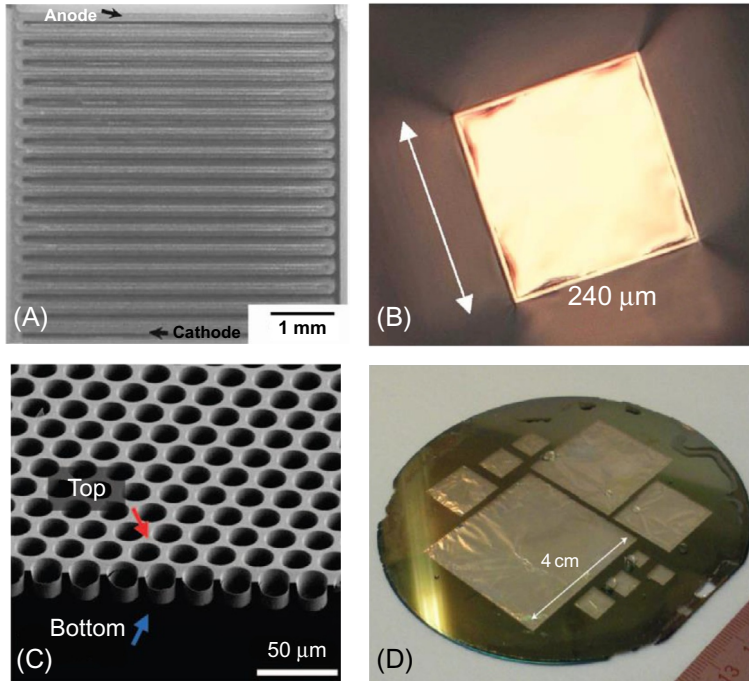

Fig. 2.4 MEMS-based SOFCs reported in the literature: (A) optical image of a single-chamber solid oxide fuel cell with micropatterned interdigitated electrodes presented by Ahn et al. [23]; (B) optical image of an ultrathin solid oxide fuel cells for low-temperature operation by Huang et al. [24]; (C) scanning electron microscope image of a solid oxide fuel cell with corrugated thin-film electrolyte by Su et al. [25]; (D) optical image of scalable nanostructured membranes for solid-oxide fuel cells by Tsuchiya et al. [26].

2.4 Biofuel cells

2.4.1 Operating principle of biofuel cells

The operating principles of biofuel cells are similar to other types of fuel cells except that the biofuel cells contain biological entities involved in energy conversion. Two main biofuel cells have been studied in the MEMS-based fuel cell community: enzymatic fuel cells [31] and MFCs [32]. The former utilizes enzymes for a catalyst while the latter utilizes microbes as a catalyst. As both share similar operation principles, we mainly discuss MFCs in this chapter.

MFCs are defined as an energy converter that directly converts the chemical energy of biomass to electrical energy with the aid of catalytic reactions of specific species of microbes named exoelectrogens, or air-breathing bacteria [3].

The most important promise of MFCs is that they convert biomass directly to electricity. As biomass is a carbon-neutral fuel; the MFC is carbon neutral and renewable. Furthermore, biomass is one of the most important sources of energy supply to society. According to a report in 2012, biomass is the largest renewable energy source in use, accounting for ~10% (5×10^{19} J) of the world's total primary energy source [33], which is equivalent to a power of 1.59 TW, 64.5% of total worldwide electricity net generation [34].

Another important promise of MFC is that it is often utilized to process wastewater besides generating electricity. According to a report, biomass in wastewater contains $\sim 1.5 \times 10^{11}$ kW h of potential energy, equivalent to 17 GW, while processing the wastewater consumes 15 GW. Thus, a net power of 2 GW is generated, making the wastewater treatment self-sustainable.

2.4.2 Challenges and promises associated with MEMS-based MFCs

2.4.2.1 Challenges

Although MFCs have been implemented during the past 15 years and significant improvements have been achieved, there are still a few challenges that need to be mitigated. The most critical challenges are low current, power density, and low output voltage.

Although the power density of MFCs has improved by several orders of magnitude, the most critical challenge of MFCs to date is still the low-power density. The highest power density of all MFCs is 6.86 W m^{-2}, and it is 2–3 orders of magnitudes lower than the power density of PEMFC and SOFC described in the section above. The low-power density is mainly due to the high internal resistance and high areal resistivity (areal resistivity is internal resistance normalized in a specific electrode surface area). According to Ren et al. [35], the areal resistivity of a MFC can be subdivided as follows:

$$r_i = r_a + r_c + r_m + r_e \tag{2.4}$$

where r_i is the total areal resistivity and r_a, r_c, r_m, and r_e are areal resistivities of the anode, cathode, ion exchange membrane, and electrolyte, respectively. As discussed

in Ren et al. [35], the areal resistivity is in the magnitude of 1 kΩ cm^2, which is high and dominates the total areal resistivity. Thus, it is critical to reduce the anode resistivity.

Similar to PEMFC and SOFC, the output voltage of MFCs is rather low; according to the section above, the open circuit voltage of a MFC is 1.08 V, assuming acetate is used as anolyte and oxygen is used as catholyte. During operation, the output voltage of MFCs is even lower, normally in the range of 0.4–0.6 V for maximum power production. On the contrary, the majority of loads require a minimum input voltage of 0.9–2.5 V. As a result, there is a gap between the output voltages of MFCs versus the input voltages of loads; therefore, connecting MFC stacks in a series is necessary. However, according to many previous reports, when several MFCs are connected in a series and the power output of one or a few MFCs are lower than others, the voltage of one or a few cells is reversed by others, resulting in no power output; this is a phenomenon called voltage reversal [36,37]. Voltage reversal will usually cause MFCs to not function, so other approaches to improve the output voltage of MFCs must be considered.

2.4.2.2 Promises

Despite the challenges listed in Section 2.4.2.1, MEMS-based MFCs offer significant promise to mitigate those challenges.

According to Ren et al. [3], as the dimension of MFCs reduces, the MEMS-based MFCs have the advantages of a reduced Reynolds number and improved mass transfer. With a higher mass transfer of biomass and buffer, the biofilm has a higher catalytic activity for biomass oxidation, which is beneficial for the power density improvement and anode areal resistivity reduction, as shown in Fig. 2.5.

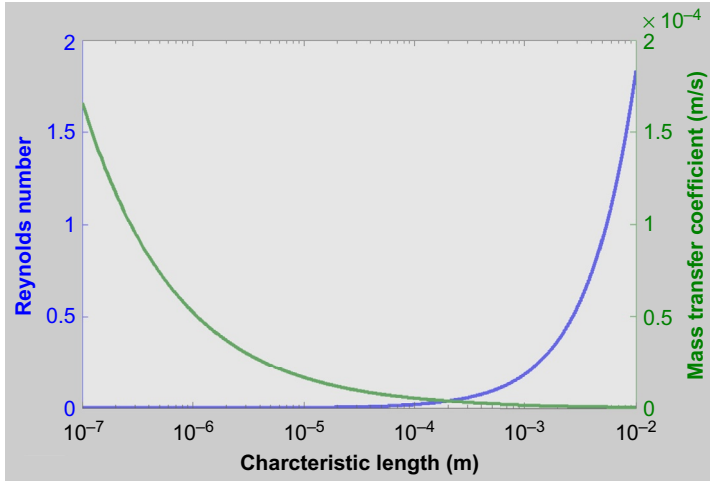

Fig. 2.5 The relationship between the Reynolds number and mass transfer coefficient versus characteristic length. As the characteristic length of an MFC reduces, the Reynolds number reduces while the mass transfer coefficient increases [3].

One of the most important advantages of miniaturization is the increased surface area to volume ratio (SAV). As the MFC scales down, the SAV increases. According to Ren et al. [3], Eq. (2.5) calculates the areal and volumetric power density:

$$p_{\max,\text{areal}} = \frac{P_{\max}}{A} = \frac{E_{\text{OCV}}^2}{4R_i \cdot A}, \quad p\max_{,\text{volumetric}} = \frac{P_{\max}}{V} = \frac{E_{\text{OCV}}^2}{4R_i \cdot V} = \frac{E_{\text{OCV}}^2}{4R_i \cdot A} \cdot \text{SAV} \tag{2.5}$$

where $p_{\max,\text{areal}}$ is the maximum areal power density, $p_{\max,\text{volumetric}}$ is the maximum volumetric power density, $P_{\max}$ is the maximum power output, A is the anode area, V is the chamber volume, E_{OCV} is the open circuit voltage, R_i is the internal resistance, and SAV is the surface area to volume ratio. As a result, as the MFC scales down, the areal power density remains unchanged while the volumetric power density increases linearly with SAV. This is another major advantage of MEMS-based MFCs.

The third advantage of MEMS-based MFCs is that the microfabrication in MEMS-based MFCs enables the fabrication of MFCs with identical dimensions. As a result, when MFC stacks with multiple MEMS-based MFCs are in operation, individual MFCs obtain similar power density, thus mitigating the voltage reversal problem [3].

2.4.3 Performance enhancement via MEMS technology

Due to the potential of MEMS-based MFCs, the last 13 years produced great advancements in MEMS MFCs. Fig. 2.6 gives an overview of representative MEMS MFCs described in the literature. The first MEMS-based MFC was invented by Chiao et al. [42] by implementing *Saccharomyces cerevisiae* as the inoculum and glucose as biomass, and the power density of this MFC was 5.72 nW m^{-2}. A few years later in 2006, they optimized the MEMS MFC by creating microfluidic channels on the anode, and in 2008, they created micropillars on PDMS substrate, both for improving the SAV [38,43]. From this, power densities of 4 mW m^{-2} and 40 W m^{-3} were achieved, which is almost six orders of magnitude improvement compared with the first MEMS MFC. In 2009 and 2011, Qian et al. [39,44] reported the first MEMS-based MFC with *Shewanella oneidensis* MR-1 as the inoculum, and a power density of 6.25 mW m^{-2} and 62.5 W m^{-3} was achieved. In 2009 and 2012, Inoue [40] and Parra and Lin [45] reported the first MEMS MFC with *Geobacter* spp. inoculum, both gold and carbon nanotube (CNT) were implemented as anodes to achieve a power density of 73.8 mW m^{-2} and 16.4 W m^{-3}.

A major performance improvement was achieved by Choi et al. in 2011. They mitigated oxygen intrusion in the anode chamber by adding L-cysteine in the anolyte and marked a power density of 47 mW m^{-2} and 2300 W m^{-3}. In 2014, Ren et al. improved mass transfer of substrate into exoelectrogen and reported a power

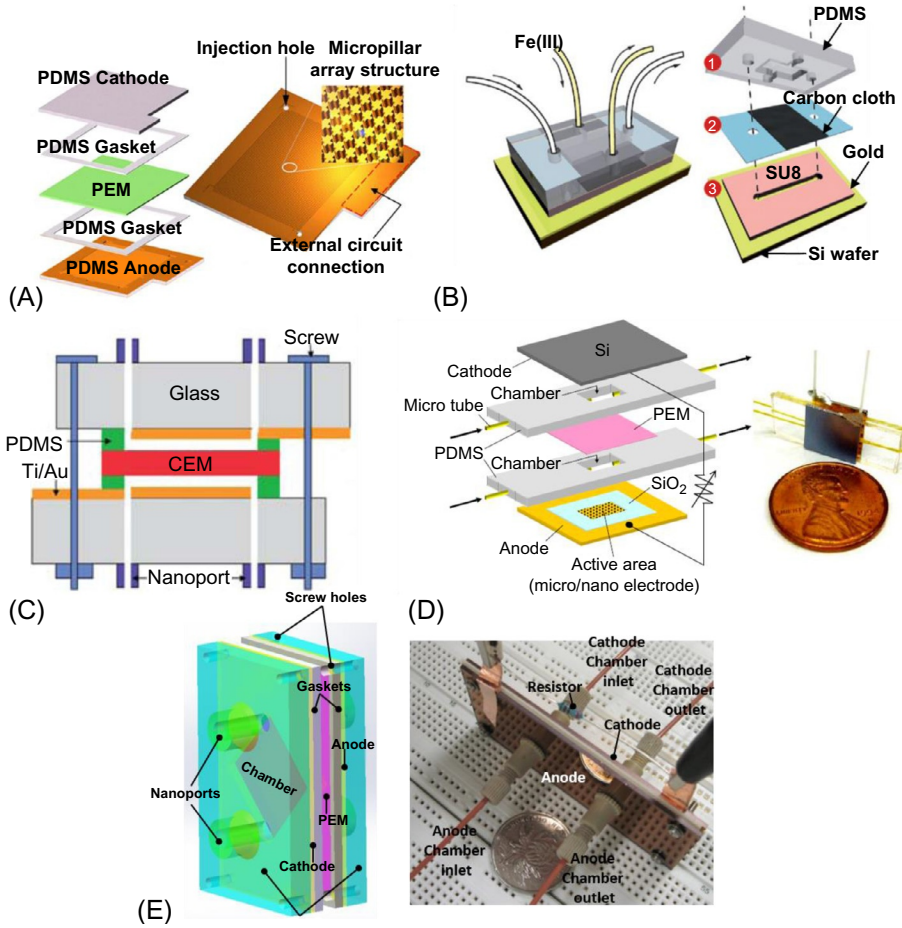

Fig. 2.6 Schematics and optical images of MEMS MFCs (A) MEMS MFC presented by Siu and Chiao [38] by applying micropillars to increase surface area to volume ratio;(B) MEMS MFC presented by Qian et al. [39], which is the first time *Shewanella oneidensis* MR-1 was implemented as the inoculum in an MEMS MFC; (C) MEMS MFC presented by Choi et al. [36], by reducing the distance between anode and cathode and mitigating oxygen leakage by adding L-cysteine; (D) MEMS MFC presented by Inoue [40], which utilizes CNT forest as an anode to reduce internal resistance; (E) MEMS MFC presented by Ren et al. [41], which improved mass transfer of substrate into exoelectrogen by investigating the scaling effect of MFCs.

density of 0.83 W m^{-2} and 3300 W m^{-3}. Additionally, in 2015, Ren et al. implemented spin-spray layer-by-layer CNT as the anode and achieved a power density of 3320 W m^{-3}. In 2016, Ren et al. adopted three-dimensional macroporous graphene scaffold as anode and the highest power density among all MFCs to date, 11,220 W m^{-3} is marked [46].

2.4.4 Electronic interface to MEMS-based MFCs

As mentioned above, connecting MFCs in a series to increase the output voltage led to a drawback of potential voltage reversal, and even in MEMS-based MFCs, voltage reversal was reported. Thus, investigating other approaches to boost the output voltage of MFC is critical. In 2015, Zhang et al. [47] developed a DC–DC converter to boost the output voltage of MFCs. They implemented a pulse frequency modulation (PFM)-type DC–DC converter in discontinuous conduction mode to address the challenges and provided a load independent output voltage. From the DC–DC converter, a high efficiency of 85% was reported at an output voltage of 0.9 V.

The operation principle of the DC–DC converter is illustrated in Fig. 2.7. When switch M_1 is on, the inductor L is charged to its maximum current by the MEMS MFC. On the other hand, when M_1 is off, the charges stored in the inductor L pass through the CMOS control rectifier (CCR) and charges the load. When the inductor current reaches ≤ 0 and output voltage $(V_{out}) > V_s$, the current path from output to inductor is blocked by the body diode of M_1. Consequently, V_{out} increases and maintains at a stable value. The switching event is automatically controlled by the supply switching module.

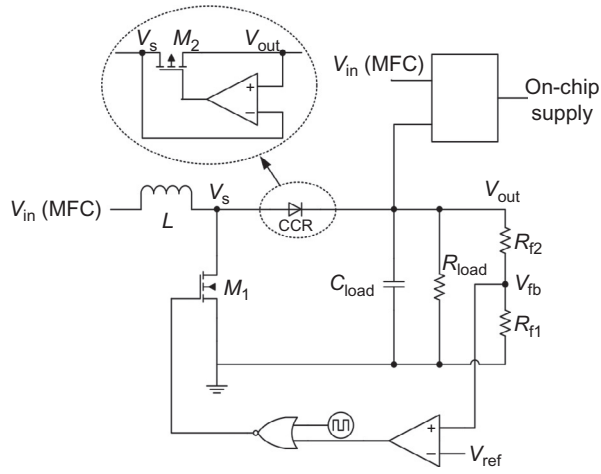

Fig. 2.7 A schematic of the operation principle of the DC–DC converter by Zhang et al. [47].

The DC–DC converter is manufactured by mixed-mode/RF UMC 0.18 μm technology, and Fig. 2.8 shows an optical image of the fabricated prototype. It is implemented on an MEMS MFC with a CNT-based anode to boost the output voltage, as shown in Fig. 2.8. As shown in Fig. 2.9, the efficiency of the converter as a function on output load is characterized at an output voltage of 0.9, 1.05, and 1.2 V. At a load of 9 μW, a high efficiency of 85% is reported when the output voltage is 0.9 V. Thus, this DC–DC converter may be widely implemented in MFCs to boost output voltage for low-power electronics.

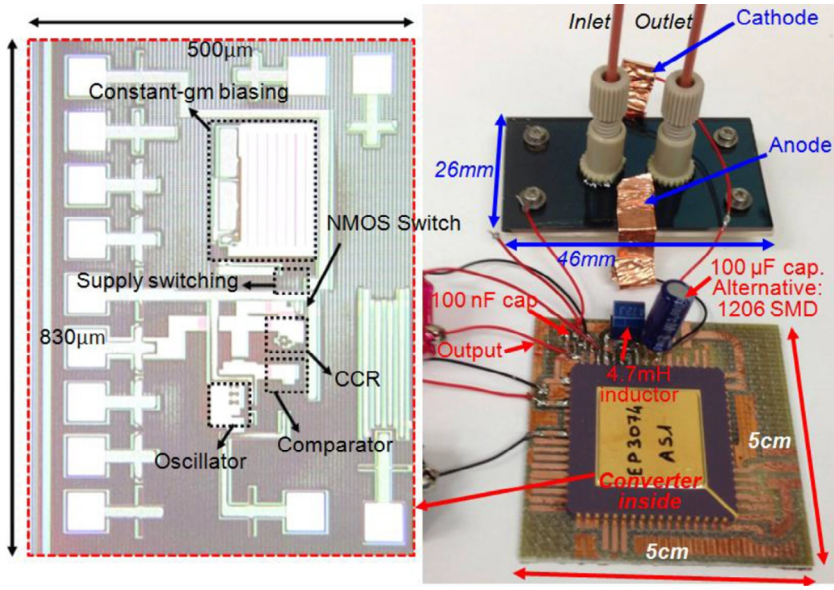

Fig. 2.8 Optical photograph of the DC–DC converter.

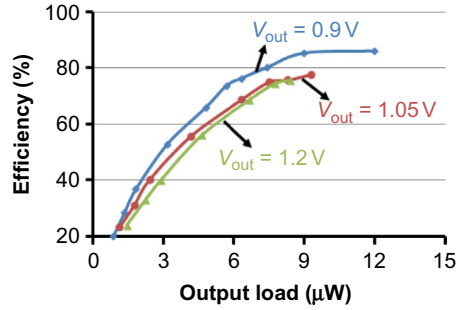

Fig. 2.9 Efficiency measurement of the DC–DC converter at three output voltages of 0.9, 1.05, and 1.2 V, respectively.

2.4.5 Supercapacitor

Although the maximum power density of MFCs successfully improved to be 0.83 W m^{-2}, it is still ~3–4 orders of magnitude lower than PEMFC and SOFC. In order to boost the power density of MFCs, Ren et al. [41] presented a microbial supercapacitor to boost the power density by 2–3 orders of magnitude. The operation principle of the microbial supercapacitor is illustrated in Fig. 2.10. A high-speed switch is implemented to control the charge/discharge of the supercapacitor. When the switch is off, the exoelectrogen breaks down acetate, generates electrodes, and stores electrons inside the biofilm. Once the switch is on, the electrons are quickly released to the

cathode, resulting in a very high-power density. Fig. 2.11 shows the output current density versus time for a microbial supercapacitor, and a very high current density of 531.2 A m^{-2} and a power density of 197.5 W m^{-2} are obtained. Thus, the power density of the microbial supercapacitor improves the current and power density by up to three orders of magnitude.

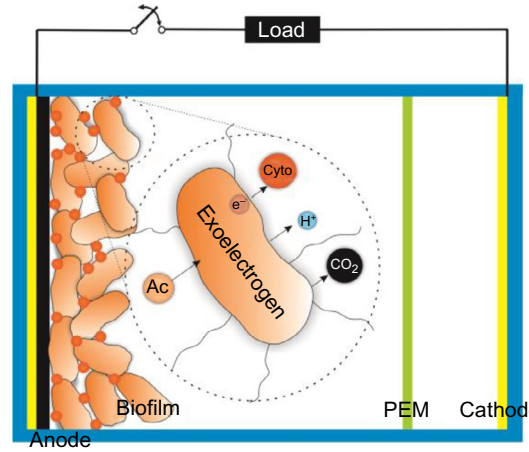

Fig. 2.10 A schematic of the operation principle of the microbial supercapacitor.

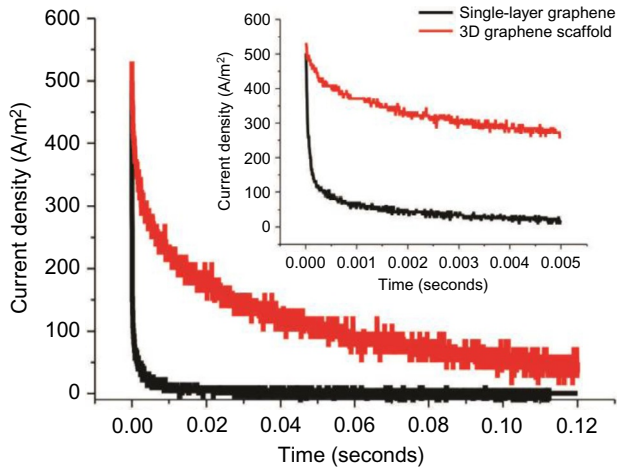

Fig. 2.11 Output current versus time of the discharging profile of the microbial supercapacitor, showing the high output current of the microbial supercapacitor.

Besides the high output current and power density, cycle stability of the microbial supercapacitor was also demonstrated in Fig. 2.12, showing a cycle stability of one million, which is believed to be due to the excellent mechanical and electrochemical stability of 2D graphene film as well as the robust, self-immobilized, and self-regenerating *Geobacter*-enriched biofilm [41]; thus, it is believed the microbial supercapacitor may find huge potentials for powering electronics.

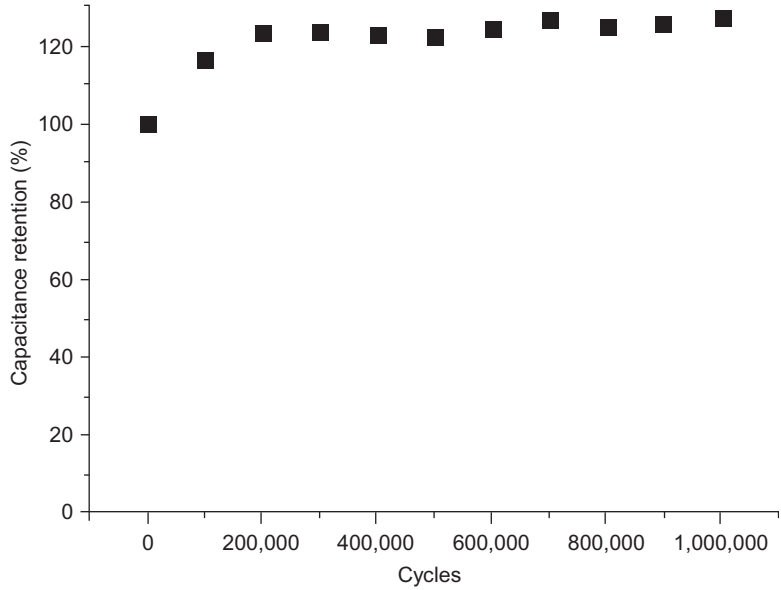

Fig. 2.12 Cycle stability of the microbial supercapacitor. The microbial supercapacitor successfully demonstrates cycle stability of 1 million cycles.

2.5 Conclusion

Based on the discussion above, the MEMS-based fuel cells, including PEMFC, SOFC, and MFCs, have all demonstrated advantages due to miniaturization. They are able to deliver a power density of 1950 W m^{-2}, 13,400 Wm^2, and 0.83 W m^{-2} respectively. Therefore, MEMS-based fuel cells are able to be implemented in different applications for wireless systems. For instance, MEMS-based PEMFC and SOFC may be implemented as power supplies for high-power wireless systems that consume a power of 100 mW, while MEMS-based MFCs may be implemented as power supplies for sub-100 μW low-power wireless systems. One potential application for MEMS-based MFC is the unattended maintenance-free power sources for environmentally hostile conditions.

References

[1] J. Garbak, VIII.0 Technology validation sub-program overview, FY 2010 annual progress report.
[2] S. Curtin, J. Gangi, R. Skukowski, The business case for fuel cells 2013: reliability, resiliency and savings, Fuel Cell (2013).
[3] H. Ren, H.-S. Lee, J. Chae, Miniaturizing microbial fuel cells for potential portable power sources: promises and challenges, Microfluid. Nanofluid. 13 (2012) 353–381.
[4] J. Chae, H. Kulah, K. Najafi, A monolithic three-axis micro-g micromachined silicon capacitive accelerometer, J. Microelectromech. Syst. 14 (2005) 235–242.

[5] N. Yazdi, F. Ayazi, K. Najafi, Micromachined inertial sensors, Proc. IEEE 86 (1998) 1640–1659.
[6] J. Liu, Y.-C. Tai, C.-M. Ho, MEMS for pressure distribution studies of gaseous flows in microchannels, in: Proceedings of the IEEE Micro Electro Mechanical Systems, 1995.
[7] D. Dudley, W.M. Duncan, J. Slaughter, Emerging digital micromirror device (DMD) applications, Micromachining and Microfabrication, International Society for Optics and Photonics, Bellingham, WA, 2003.
[8] N. Xu, et al., A wireless sensor network for structural monitoring, in: Proceedings of the 2nd International Conference on Embedded Networked Sensor Systems, ACM, Baltimore, MD, 2004.
[9] E. Welbourne, et al., Building the internet of things using RFID: the RFID ecosystem experience, IEEE Internet Comput. 13 (2009) 48–55.
[10] S. Roundy, D. Steingart, L. Frechette, P. Wright, J. Rabaey, Power sources for wireless sensor networks, Wireless Sensor Networks, Springer, Berlin, Heidelberg, 2004.
[11] T. Handa, S. Shoji, S. Ike, S. Takeda, T. Sekiguchi, A very low-power consumption wireless ECG monitoring system using body as a signal transmission medium, in: 1997 International Conference on Solid State Sensors and Actuators, TRANSDUCERS'97 Chicago, IEEE, Washington, DC, 1997.
[12] J. Yeom, et al., Microfabrication and characterization of a silicon-based millimeter scale, PEM fuel cell operating with hydrogen, methanol, or formic acid, Sensors Actuators B Chem. 107 (2005) 882–891.
[13] P. Costamagna, S. Srinivasan, Quantum jumps in the PEMFC science and technology from the 1960s to the year 2000: Part I. Fundamental scientific aspects, J. Power Sources 102 (2001) 242–252.
[14] S. Lee, et al., Design and fabrication of a micro fuel cell array with "flip-flop" interconnection, J. Power Sources 112 (2002) 410–418.
[15] K. Shah, W. Shin, R. Besser, A PDMS micro proton exchange membrane fuel cell by conventional and non-conventional microfabrication techniques, Sensors Actuators B Chem. 97 (2004) 157–167.
[16] X. Zhang, et al., A preliminary study of a miniature planar 6-cell PEMFC stack combined with a small hydrogen storage canister, J. Power Sources 166 (2007) 441–444.
[17] T. Kim, S. Kwon, MEMS fuel cell system integrated with a methanol reformer for a portable power source, Sensors Actuators A Phys. 154 (2009) 204–211.
[18] H.-C. Peng, C.-N. Wang, T.-K. Yeh, Y.-C. Su, C. Pan, F.-G. Tseng, A high efficient micro-proton exchange membrane fuel cell by integrating micro-nano synergical structures, J. Power Sources 225 (2013) 277–285.
[19] J. Lee, T. Kim, Micro space power system using MEMS fuel cell for nano-satellites, Acta Astronaut. 101 (2014) 165–169.
[20] S. Kelley, G. Deluga, W. Smyrl, A miniature methanol/air polymer electrolyte fuel cell, Electrochem. Solid-State Lett. 3 (2000) 407–409.
[21] S.-C. Yao, et al., Micro-electro-mechanical systems (MEMS)-based micro-scale direct methanol fuel cell development, Energy 31 (2006) 636–649.
[22] R.M. Ormerod, Solid oxide fuel cells, Chem. Soc. Rev. 32 (2003) 17–28.
[23] S.-J. Ahn, J.-H. Lee, J. Kim, J. Moon, Single-chamber solid oxide fuel cell with micro-patterned interdigitated electrodes, Electrochem. Solid-State Lett. 9 (2006) A228–A231.
[24] H. Huang, M. Nakamura, P. Su, R. Fasching, Y. Saito, F.B. Prinz, High-performance ultrathin solid oxide fuel cells for low-temperature operation, J. Electrochem. Soc. 154 (2007) B20–B24.
[25] P.-C. Su, C.-C. Chao, J.H. Shim, R. Fasching, F.B. Prinz, Solid oxide fuel cell with corrugated thin film electrolyte, Nano Lett. 8 (2008) 2289–2292.

[26] M. Tsuchiya, B.-K. Lai, S. Ramanathan, Scalable nanostructured membranes for solid-oxide fuel cells, Nat. Nanotechnol. 6 (2011) 282–286.
[27] V. Srikar, K.T. Turner, T.Y.A. Ie, S.M. Spearing, Structural design considerations for micromachined solid-oxide fuel cells, J. Power Sources 125 (2004) 62–69.
[28] C.D. Baertsch, et al., Fabrication and structural characterization of self-supporting electrolyte membranes for a micro solid-oxide fuel cell, J. Mater. Res. 19 (2004) 2604–2615.
[29] A. Bieberle-Hütter, et al., A micro-solid oxide fuel cell system as battery replacement, J. Power Sources 177 (2008) 123–130.
[30] C.-C. Chao, C.-M. Hsu, Y. Cui, F.B. Prinz, Improved solid oxide fuel cell performance with nanostructured electrolytes, ACS Nano 5 (2011) 5692–5696.
[31] H.J. Kim, H.S. Park, M.S. Hyun, I.S. Chang, M. Kim, B.H. Kim, A mediator-less microbial fuel cell using a metal reducing bacterium, *Shewanella putrefaciens*, Enzyme Microb. Technol. 30 (2002) 145–152.
[32] H. Liu, B.E. Logan, Electricity generation using an air-cathode single chamber microbial fuel cell in the presence and absence of a proton exchange membrane, Environ. Sci. Technol. 38 (2004) 4040–4046.
[33] IE Agency, Medium-term renewable energy market report, 2014.
[34] IE Statistics, International Energy Statistics—electricity, 2012.
[35] H. Ren, et al., A high power density miniaturized microbial fuel cell having carbon nanotube anodes, J. Power Sources 273 (2015) 823–830.
[36] S. Choi, J. Chae, An array of microliter-sized microbial fuel cells generating 100 μW of power, Sensors Actuators A Phys. 177 (2012) 10–15.
[37] S.-E. Oh, B.E. Logan, Voltage reversal during microbial fuel cell stack operation, J. Power Sources 167 (2007) 11–17.
[38] C.P.B. Siu, M. Chiao, A microfabricated PDMS microbial fuel cell, J. Microelectromech. Syst. 1057-7157, 17 (2008) 1329–1341.
[39] F. Qian, M. Baum, Q. Gu, D.E. Morse, A 1.5 μL microbial fuel cell for on-chip bioelectricity generation, Lab Chip 9 (2009) 3076–3081.
[40] S. Inoue, Structural optimization of contact electrodes in microbial fuel cells for current density enhancements, Sens. Actuators A Phys. 177 (2012) 7.
[41] H. Ren, et al., Regulating the respiration of microbe: a bio-inspired high performance microbial supercapacitor with graphene based electrodes and its kinetic features, Nano Energy 15 (2015) 697–708.
[42] M. Chiao, K.B. Lam, Y. Su, L. Lin, A miniaturized microbial fuel cell, in: Solid-State Sensor, Actuator and Microsystems Workshop, 2002.
[43] M. Chiao, K.B. Lam, L. Lin, Micromachined microbial and photosynthetic fuel cells, J. Micromech. Microeng. 16 (2006) 2547.
[44] F. Qian, Z. He, M.P. Thelen, Y. Li, A microfluidic microbial fuel cell fabricated by soft lithography, Bioresour. Technol. 102 (2011) 5836–5840.
[45] E. Parra, L. Lin, Microbial fuel cell based on electrode-exoelectrogenic bacteria interface, in: IEEE 22nd International Conference on Micro Electro Mechanical Systems, 2009, MEMS 2009, IEEE, Washington, DC, 2009.
[46] H. Ren, H. Tian, C.L. Gardner, T.L. Ren, J. Chae, A miniaturized microbial fuel cell with three-dimensional graphene macroporous scaffold anode demonstrating a record power density of over 10,000 Wm^{-3}, Nanoscale 8 (2016) 3539–3547.
[47] X. Zhang, H. Ren, S. Pyo, J.-I. Lee, J. Kim, J. Chae, A high-efficiency DC–DC boost converter for a miniaturized microbial fuel cell, IEEE Trans. Power Electron. 30 (2015) 2041–2049.